Fast Multislice Mapping of the Myelin Water Fraction Using Multicompartment Analysis of T_2^* Decay at 3T: A Preliminary Postmortem Study

Yiping P. Du,[1,2*] Renxin Chu,[1] Dosik Hwang,[1] Mark S. Brown,[2] Bette K. Kleinschmidt-DeMasters,[3–5] Debra Singel,[1] and Jack H. Simon[2,6]

Quantitative mapping of the myelin water content can provide significant insight into the pathophysiology of several white matter diseases, such as multiple sclerosis and leukoencephalopathies, and can potentially become a useful clinical tool for early diagnosis of these diseases. In this study, multicompartment analysis of T_2^* decay (MCAT2*) was used for the quantitative mapping of myelin water fraction (MWF). T_2^* decay of each voxel at multiple slice locations was acquired in fixed human brains using a multigradient-echo (MGRE) pulse sequence with alternating readout gradient polarities. Compared to prior techniques using Carr-Purcell-Meiboom-Gill (CPMG) acquisition, the MGRE acquisition approach has: 1) a very short first echo time (≈2 ms) and echo-spacing (≈1 ms), which allows for the acquisition of multiple sampling points during the fast decay of the myelin water signal; 2) a low RF duty cycle, which is especially important for achieving acceptable specific absorption rate (SAR) levels at high field strengths. Multicompartment analysis was then applied to the T_2^* decay in each pixel using a 3-pool model of white matter to detect the signal arising from the myelin water, myelinated axonal water, and mixed water compartments. Magn Reson Med 58:865–870, 2007. © 2007 Wiley-Liss, Inc.

Key words: myelin water fraction; multicompartment analysis; demyelination; multiple sclerosis; postmortem

While conventional MRI methods are sensitive to the various pathologies affecting white matter in the central nervous system, it provides relatively nonspecific information about the nature of the underlying pathology. One approach developed based on multicompartment analysis of T_2 decay provides quantitative measurements of myelin water fraction (MWF) (1). Quantitative mapping of the MWF is a direct indicator of the integrity of the myelin sheath and can provide valuable insights into the pathology of focal and diffuse white matter (WM) diseases, such as in multiple sclerosis (MS).

One technique for quantitative in vivo mapping of the MWF was presented by MacKay et al. (2). In this technique the time course of T_2 decay was acquired using a 32-echo single-slice Carr-Purcell-Meiboom-Gill (CPMG) sequence with composite $90°_x$-$180°_y$-$90°_x$ refocusing pulses (3) and big crusher gradients around the refocusing pulses (4). A nonnegative least squares (NNLS) algorithm was used to estimate the MWF from the short T_2 decay compartment (5). This technique has very successfully demonstrated the merit of quantitative MWF measurement in the study of MS (6). However, there are some limitations associated with this technique. First, it is difficult to further shorten the first echo time (TE1) and echo spacing (ES) with this pulse sequence, since the durations of the nonselective refocusing pulses and the crusher gradients (4) substantially increase the minimum TE1 and ES. With the TE1 and ES values typically used, the myelin water signal is effectively detected only in the first 2–3 measurements (i.e., first 2–3 echoes), leading to compromised accuracy in estimating the MWF using multicompartment analysis. For example, the myelin water signal with a T_2 of 15 ms is reduced to 51% at the first echo, 26% at the second echo, and 13.5% at the third echo with TE1 = 10 ms and ES = 10 ms. An average of four scans is usually required (at 1.5T) with a total scan time of 25–28 min to increase the signal-to-noise ratio (SNR) for data analysis. Second, this CPMG technique can only acquire one slice because of the use of nonselective refocusing pulses, making it difficult to analyze multiple lesions that cannot be evaluated by a single slice. While this technique has proven to be effective in detecting demyelination in MS lesions and normal-appearing white matter (NAWM), the lack of volume coverage, as well as the long image acquisition time, has severely limited the application of this technique in the study of myelination and demyelination. Third, the high specific absorption rate (SAR) used in the CPMG acquisition can severely limit its application in routine human scans especially at high field strengths (i.e., 3T and higher). Finally, the accuracy of the MWF measurements can be compromised because the T_2 of myelin water is not well defined using the NNLS algorithm (5). For the T_2 range of myelin water ($10 \text{ ms} < T_2 < 50 \text{ ms}$) used in the NNLS algorithm, a substantial portion of signal from myelinated axon water ($T_2 \approx 40$ ms, at 1.97 (7); $T_2 = 29.7$ ms in frontal WM samples at 7T (8)) could be misclassified

[1]Department of Psychiatry, University of Colorado Health Sciences Center, Denver, Colorado.
[2]Department of Radiology, University of Colorado Health Sciences Center, Denver, Colorado.
[3]Department of Pathology, University of Colorado Health Sciences Center, Denver, Colorado.
[4]Department of Neurology, University of Colorado Health Sciences Center, Denver, Colorado.
[5]Department of Neurosurgery, University of Colorado Health Sciences Center, Denver, Colorado.
[6]Imaging Department, Portland Veterans Administration Medical Center, Portland. Oregon.

Presented in part in: Proceedings of the 14th Annual Meeting of ISMRM, Seattle, 2006.
Grant sponsor: National Multiple Sclerosis Society; Grant numbers: pilot grant PP1260 (to Y.P.D.) and RG 3307-A-1 (to J.H.S.).

*Current address and correspondence to: Yiping P. Du, PhD, Departments of Psychiatry and Radiology, University of Colorado Health Sciences Center, Building 400, 12469 East 17th Pl., Aurora, CO 80010.
E-mail: Yiping.Du@UCHSC.edu

Received 15 December 2006; revised 8 July 2007; accepted 12 August 2007.
DOI 10.1002/mrm.21409
Published online in Wiley InterScience (www.interscience.wiley.com).

into the myelin water signal, leading to a possible overestimation of the MWF.

The purpose of our current study was to develop a new imaging technique and data analysis approach, referred as MCAT2*, for quantitative multislice mapping of the MWF in human brains in a clinically acceptable imaging time. More specifically, our objectives were: 1) to substantially increase the number of measurements before the decay of the myelin water signal; 2) to increase the volume coverage and reduce the imaging time by using multislice data acquisition; 3) to reduce the SAR in data acquisition; and 4) to reduce the chance of misclassifying myelinated axon water signal into the myelin water signal by applying a more restricted constrain of the T_2^* range of the myelin water signal in multicompartment analysis. To achieve these objectives a multigradient-echo (MGRE) pulse sequence, in which a train of readout gradients with alternating polarity, was used for data acquisition in this study. By using this sequence we can reduce TE1 to 2.1 ms and ES to 1.1 ms in acquiring images with a 256 × 256 matrix. Using these shortened TE1 and ES values, the myelin signal with a T_2^* of 10 ms will be at 81% at the first measurement and 24% at the 12th measurement (i.e., 12th echo). The MWF is calculated using multicompartment analysis with a 3-pool model of WM (7).

MATERIALS AND METHODS

Three-Pool Model

In the 3-pool model, WM tissue consists of a myelin (my) water pool, a myelinated axon (ma) water pool, and a mixed (mx) water pool. This model was originally applied to the measurements of T_2 decay, with the estimated T_2 of 10 ms for the my pool, 40 ms for the ma pool, and 130 ms for the mx pool for frontal WM at 1.9T (7). In this study, the use of the 3-pool model was extended to the measurement of T_2^* decay with seven unknowns:

$$S(t) = A_{my}e^{-t/T_{2,my}^*} + A_{ma}e^{-t/T_{2,ma}^*} + A_{mx}e^{-t/T_{2,mx}^*} + A_{bl} \quad [1]$$

where the A_{my}, A_{ma}, and A_{mx} represent the amplitude of the signals arising from 3 water pools, respectively, and A_{bl} represents any residual baseline signal. After fitting the measured signal decay with the 3-pool model, MWF was estimated as:

$$MWF = A_{my}/(A_{my} + A_{ma} + A_{mx}). \quad [2]$$

Data Acquisition and Image Reconstruction

A postmortem brain acquired from an older woman with long-standing chronic inactive MS was scanned, as were two other postmortem brains from non-MS individuals without focal lesions. The brains were fully fixed in 10% buffered formalin and then placed in a water-filled container for scan after carefully removing the air bubbles. High-order shim was performed to minimize field inhomogeneity. The T_2^* signal decay in each pixel was detected using the MGRE acquisition on a 3T MRI scanner (General Electric, Waukesha, WI) equipped with high-performance gradient coils (maximum gradient amplitude of 40 mT/m and maximum slew rate of 150 T/m/s). This pulse sequence uses a train of readout gradients with alternating polarity immediately after phase-encoding (Fig. 1), similar to the pulse sequence used in echo-planar spectroscopic imaging (9). A minimum-phase Shinnar–LeRoux excitation pulse (10) of 3.2 ms was used to minimize TE1. The echoes were acquired on both the flat-top and the readout gradient ramps in order to further shorten the TE1 and ES. Gradient spoilers were applied to all the 3 axes at the end of the readout train to destroy any residual transverse component of the magnetization. In our experiment, we acquire 126 echoes in the readout train with an image matrix of 256 × 256, TE1 of 2.1 ms, and ES of 1.1 ms. The other imaging parameters were: 20 cm field-of-view (FOV) and 5 mm slice thickness with a 1 mm gap between slices. The timing of the pulse sequence would allow for the acquisition of up to 12 slices using a repetition time (TR) of 2 sec. In this study we limited our acquisition to 5 slices with a TR of 2 sec, with an imaging time of 8.7 min, to avoid possible overheating of the gradient system through the calculation of gradient duty cycle by the pulse sequence software. The quality of the MWF maps is expected to be affected by the SNR in the acquired data. In order to estimate the minimal SNR necessary for reliable MWF mapping, we conducted a separate experiment in which data were acquired with different slice thicknesses at 2, 3, 4, and 5 mm, respectively.

The *k*-space data of each slice were reconstructed into the (x, y, t) domain on an off-line computer using reconstruction software developed in our laboratory. In order to minimize the possible adverse effects of the mismatch

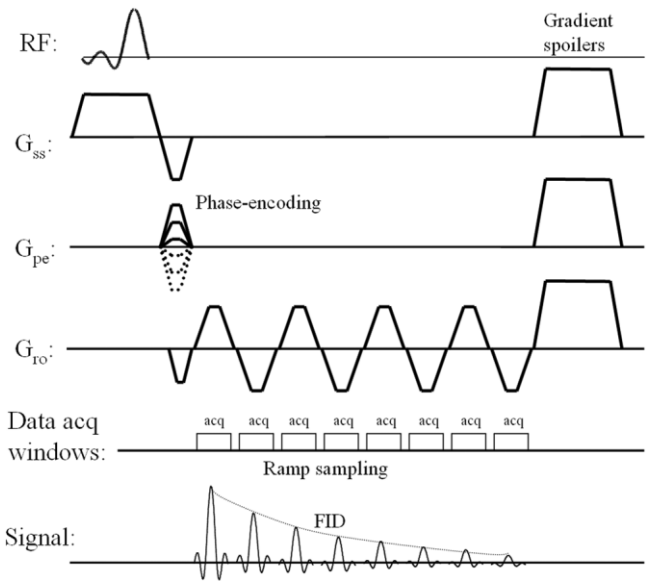

FIG. 1. The diagram of the MGRE pulse sequence in which the phase-encoding (PE) gradient lobe steps through the k_y lines. A train of readout gradients with alternating polarity was played out immediately after the phase-encoding. A minimal-phase SLR pulse was used to minimize TE1. Data were acquired on both the ramps and top of the readout gradients to reduce the echo spacing. Gradient spoilers were added at the end of the pulse sequence to reduce the residual magnetization. For simplicity, only 8 echo readouts are shown in this diagram.

between even and odd echoes on the T_2^* decay measurements, the even and odd echoes were aligned to minimize the amplitude of the spectral ghost in the water resonance (11). Inverse Fourier transform was then applied to the corrected water resonance profile to obtain the corrected T_2^* free induction decay (FID). A threshold was used to remove the region of air prior to the multicompartment analysis.

For histological preparation, sections of MS plaques corresponding to the scanned areas were embedded in paraffin wax, cut at 6 μm, and stained in standard fashion with Harris hematoxylin and eosin, Luxol fast blue-periodic Schiff stain for myelin, and modified Bielschowsky stain for axons.

Multicompartment Analysis

A quasi-Newton algorithm for multivariable optimization in Matlab (MathWorks, Natick, MA) was used to minimize the root-mean-squares error between the fitting and the measured signal relaxation. Accurate fitting requires proper selection of the T_2^* ranges for the 3 pools (i.e., from τ_{b0} to τ_{b1} for the my pool, from $\tau_{b1}$to τ_{b2} for the ma pool, and from τ_{b2} to τ_{b3} for the mx pool). We select τ_{b0} = 3 ms because a first echo time of 2.1 ms makes the fitting for any signal with a T_2^* less than 3 ms unreliable. The proper selection of τ_{b1} is especially critical for accurate MWF measurement. If τ_{b1} is set too small, a portion of myelin water signals would be misclassified as the ma signal, resulting in an underestimation of the MWF and a higher fitting error. If τ_{b1} is set too high, some portion of myelinated axon water signal would be misclassified as the my signal, resulting in an overestimation of the MWF and a higher fitting error due to the misfitting of the ma pool. In this study, we selected τ_{b1} = 16 ms, τ_{b2} = 36 ms, and τ_{b3} = 160 ms. These T_2^* endpoints were determined by repeated test fittings in which the optimal T_2^* endpoints resulted in minimal fitting error and minimal variation of the MWF estimation (i.e., $d(MWF)/d\tau_b$) in NAWM. The initial values for the fitting were 10 ms, 25 ms, 50 ms for T_2^* and 10%, 25%, 65% for the fraction in the my, ma, and mx pool, respectively. Considering the shortening of T_2 and T_2^* by the fixation of brain tissue (12), these selections of T_2^* ranges are consistent with a previous experiment conducted using frontal WM samples at 7T in which T_2 was determined to be 8.2 ms for the my pool, 29.7 ms for the ma pool, and 66.9 ms for the mx pool (8).

RESULTS

Five MWF maps from the fixed MS brain (top) and T_2-FLAIR images acquired at the same slice locations (bottom) are shown in Fig. 2. The myelin water signal was reliably detected in regions of NAWM in all slices. The MWF was substantially reduced, or nearly undetectable at the locations of focal MS lesions, as indicated by arrows. Several small lesions shown in the T_2-FLAIR images were well depicted in the MWF maps (e.g., the lesions indicated by the arrows at the fourth slice). Expected differences in myelin content of normal regions of gray matter (GM) and WM are also apparent in these MWF maps.

The mean MWF was measured in several NAWM regions of the fixed brain. The mean MWF was 12.0% at the genu of corpus callosum, 15.2% at internal capsule, 8.9% at the frontal WM (FWM), and 11.2% at the posterior WM (PWM). The average of MWF in these areas was 11.0%. These measurements are consistent with previously reported MWF values in these regions (see Table 1).

Figure 3 shows the individual maps of the my pool, ma pool, and mx pool at Slice 4. The ma and mx maps show well-delineated GM, WM, and MS lesions. The T_2^* of GM appears to be in the range of the ma and mx pools, resulting in higher intensity in the ma and mx maps. The center of a lesion, as indicated by a short arrow, appears to have much lower intensity in the my and ma pools, suggesting both severe demyelination and axonal damage. The periphery of MS lesions, indicated by a long arrow, have a lower intensity in the my pool and a higher intensity in the ma pool, suggesting more demyelination than axonal damage. In addition, the center of the lesions has a higher intensity than the periphery of the lesions for the mx pool, further suggesting that axonal damage is of lesser magnitude at the periphery of these lesions. This study demonstrates that the 3-pool modeling can potentially provide a direct assessment of axonal damages in addition to demyelination.

The histopathology based on myelin stain in the region of an MS lesion is shown in Fig. 4, confirming severe

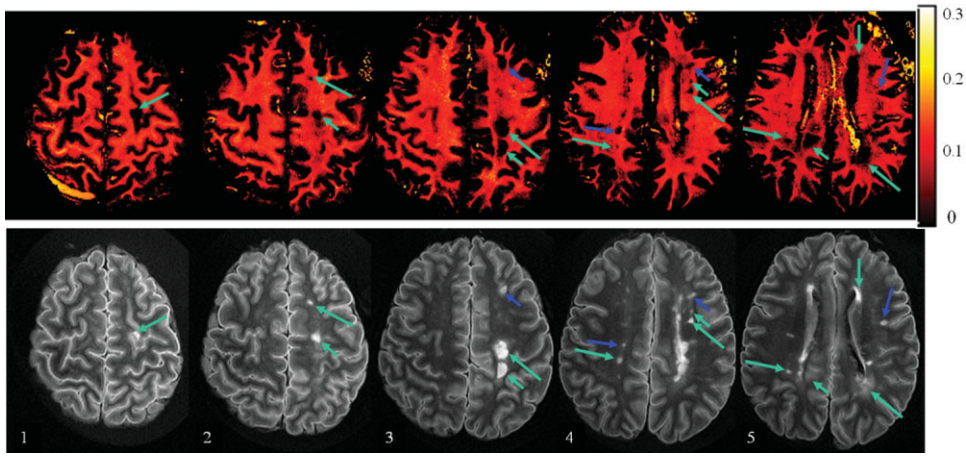

FIG. 2. MWF maps (upper panel) and T_2-FLAIR images (lower panel) acquired at the same locations. The region of MS lesions indicated by the arrows in the T_2-FLAIR images has reduced MWF.

Table 1
Comparison of Reported MWF Values and the MWF Values Obtained in This Study in Several WM Regions

ROI \ Study	Ref. 2	Ref. 13	Ref. 14	Ref. 15	Ref. 16 (1.5T)	Ref. 16 (3T)	Ref. 8	Ref. 7	Our Study
Genu of CC	10	9.86	10.1	12.35	7.3	12.1	—	—	12
Splenium of CC	—	13.05	13.3	—			—	—	—
Minor forceps	—	8.4	7.3	—	—	—	—	—	—
Major forceps	—	10.11	9.5	—	—	—	—	—	—
Internal capsule	—	15.0	15.6	12.25	9.0	12.3	—	—	15.2
Frontal WM	—	—	—	10.05	7.0	10.1	14.9	17	8.9
Posterior WM	11 (Peritrigonal)	—	—	11.85	—	—	—	—	11.2
Average WM	15.6 ± 8.1	11.28	8.9 (cNAWM)	—	—	—	—	—	11.0

demyelination of the lesion corresponding to the findings from the MWF map. The boundaries between WM and GM shown in the MWF map also matched the histopathology. The through-plane partial volume of the lesion in the MRI data may cause the lesion to appear larger in the MWF map than in the histopathology. A higher-power photomicrograph (LFB-PAS, 400×) shows totally devoid of myelin at the center of MS lesion, and the normal myelin content in NAWM outside the MS lesion.

Similar MWF maps were obtained with two other fixed brains (Fig. 5). Although no local lesions are present in these maps, expected differences in myelin content of normal regions of GM and WM are also apparent in these MWF maps.

The SNR of the images acquired at TE1 and difference slice thicknesses was estimated to be 40.8 (at 2 mm), 59.6 (at 3 mm), 83.5 (at 4 mm), and 98.9 (at 5 mm), respectively. In the SNR measurement, the noise level was calculated as the average of $M_{mean}/1.253$ and $M_{sd}/0.655$, where M_{mean} is the mean and M_{sd} is the standard deviation of the magnitude intensity measured in an air region outside the brain (17). The low level of spatial noise in the MWF maps acquired at 4 and 5 mm suggest that myelin detection was reliable with an SNR of 83.5 and above (Fig. 6). The increased level of spatial noise becomes more noticeable in the MWF map acquired at 3 mm, and unacceptable in the MWF map acquired at 2 mm.

DISCUSSION

These results demonstrate the feasibility of a new approach for quantitative mapping of myelin water content using fast multislice data acquisition and multicompartment analysis. With increased accuracy of sampling of the fast T_2^* compartment of myelin and fast multislice acquisition, this approach can potentially provide more insight into the pathology of WM diseases related to demyelination, such as MS, as well as myelination in health and disease. In addition, this technique may be useful in interrogating other water compartments, such as an hypothesized axonal water compartment, that may provide insight into axonal injury and degenerative processes, separate from demyelination. Although we have applied our new methodology to a fixed MS brain, it has the potential to be equally informative for leukoencephalopathies of either metabolic or ischemic nature since it exquisitely details areas of partial myelin loss, such as the surrounding periplaque white matter, as well as severe loss that is seen in the central portions of chronic inactive MS plaques.

Acquiring T_2^* decay is advantageous for large volume coverage because the length of sequence for each *k*-space line with the MGRE acquisition can be greatly reduced due to the fact that the T_2^* decay in WM is approximately twice faster than the T_2 decay. With a faster decay of the transverse relaxation, the residual transverse component of the magnetization will be more effectively spoiled at the end of the sequence. In MacKay and Whittall's implementation, 32 echoes were acquired with a duration of 320 ms for each *k*-space line (2). In our implementation, 126 echoes were acquired in less than 150 ms for each *k*-space line. This reduced data acquisition duration would allow us to acquire one *k*-space line for up to 12 slices with a TR of 2 sec in our study if the number of slices was not limited by the gradient duty cycle.

It is desirable to conduct the MWF mapping studies at high magnetic field strengths (3T and higher) for the SNR benefit. The proposed MCAT2* technique is more suitable at high magnetic field strengths than the CPMG technique

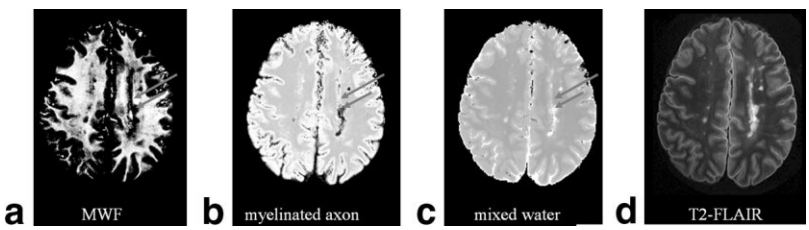

FIG. 3. The maps of the 3 pools **(a–c)** show excellent delineation of MS lesions, WM, and GM. The T_2-FLAIR image acquired at the same slice location is shown in **(d)** for the location of the lesions. At a region indicated by the long arrow, the decreased intensity in **(a)** and increased intensity in **(b)** suggest the dominance of the demyelination process. At a central region of a lesion indicated by a short arrow, the decreased intensity in both **(a)** and **(b)** suggest the occurrence of both demyelination and axonal damage.

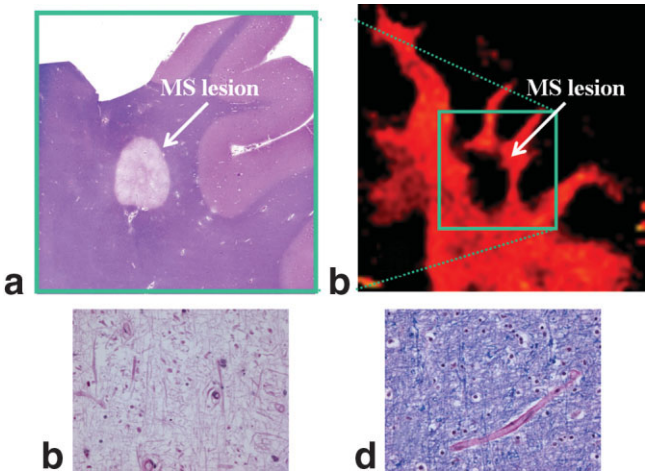

FIG. 4. The histopathology of the MS lesion **(a)** confirms the demyelination at the region where the MWF map **(b)** at the third slice in Fig. 2 shows severely decreased intensity, as indicated by the pale region within the center of the rectangular area. A higher-power photomicrograph (LFB-PAS, 400×) shows totally devoid of myelin at the center of MS lesion **(c)**, and the normal myelin content in NAWM outside the MS lesion **(d)**.

for two reasons. First, the T_2^* data acquisition employs only one excitation RF pulse (≤90°) in the sequence and has a very low SAR. In contrast, the T_2 data acquisition employs a train of refocusing pulses and, therefore, its clinical application at high field strengths can be severely limited due to its high SAR. Second, the length of echo train can be further shortened in T_2^* acquisition because of the reduced T_2^* at higher field strengths, while T_2 is more or less independent of the field strength. The decrease of T_2^* allows a reduced length of echo train without increasing the residual of transverse magnetization at the end of the sequence.

The imaging time can be further reduced by using a shorter TR without significant reduction of the myelin water signal because of its short T_1 value ($T_{1,my}$ = 350 ms at 1.9T) (8). The signals from the ma and mx pools, on the other hand, will experience more T_1 partial saturation due to their relatively long T_1 values, leading to an overestimation of the MWF ($T_{1,ma}$ = 850 ms and $T_{1,mx}$ = 2800 ms at 1.9T) (8). The suppression of the signals from the ma

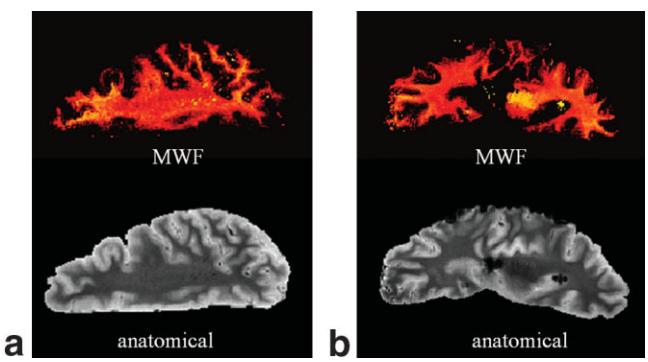

FIG. 5. Representative MWF maps of two other fixed brains **(a,b)**. These maps show higher MWF in the white matter regions.

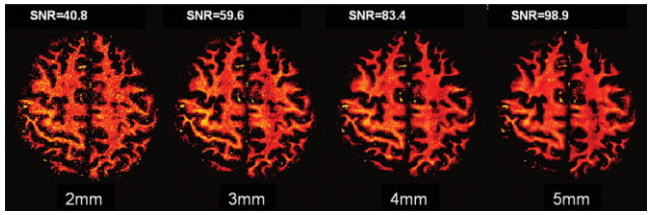

FIG. 6. MWF maps with slice thickness of 2, 3, 4, and 5 mm. The SNR of the images acquired at TE1, shown at the top of each map, was approximately proportional to the slice thickness. The MWF map acquired at 4 mm slice thickness is comparable to that acquired at 5 mm slice thickness. The spatial noise in the MWF maps becomes more noticeable at 3 mm slice thickness and unacceptable at 2 mm slice thickness.

and mx pools in the T_2^* decay measurement may possibly enhance the detection of the myelin water signal in the multicompartment analysis. However, T_1 correction will be necessary to improve the accuracy in the MWF mapping at short TRs.

Accurate multicompartment analysis for MWF mapping requires high SNR in the MRI data. In published studies of MWF mapping using the CPMG data acquisition and NNLS analysis, an average of four scans is required to obtain sufficient SNR at 1.5T even at a relatively low spatial resolution with a voxel volume of 7.39 mm^3 (i.e., 256 × 128 matrix, 22 cm FOV, and 5 mm slice thickness) (2). The increase of the imaging time (i.e., 26 min) due to the averaging of multiple scans makes the technique not suitable for routine clinical studies. We expect an improved SNR efficiency with the MGRE acquisition. By eliminating the need for refocusing pulses, a much higher portion of time in the echo train is used for data acquisition in the MGRE sequence than in the CPMG sequence, resulting in a higher SNR efficiency in the MGRE data. In addition, the multislice acquisition further increases the SNR efficiency in the MGRE acquisition. This postmortem study indicates that an imaging protocol with a much higher spatial resolution with a voxel volume of 2.44 mm^3 (i.e., 256 × 256 matrix, 20 cm FOV, and 4 mm slice thickness) provides sufficient SNR at 3T. However, the actual SNR will be much lower with in vivo data than with postmortem data because physiological noise can substantially contribute to the total noise.

Optimal in vivo implementation of the MCAT2* approach will require consideration of several technical challenges because this MGRE acquisition is susceptible to physiological noise, especially in later echoes. Although the myelin water signal has a short decay constant and is not present in later echoes, the signal fluctuation in later echoes will compromise the overall MCAT2* fitting accuracy and adversely affect the MWF measurements. Using navigator echoes should be considered for monitoring and correcting the respiratory effect, if necessary (18).

The MGRE acquisition is also sensitive to cardiac motion. The motion of the flowing blood can introduce additional phase variation in the echo train and cause spatial and spectral ghosting. The pulsation of blood in the arteries can also introduce small brain motion, especially in locations near the arteries. Both flowing blood and pulsa-

tile brain motion can cause signal fluctuation in the images acquired at different timepoints and cause errors in the MCAT2* fitting. Flow compensation in the slice-selection gradient could be used to ease the motion artifact, with the penalty of increased TE1.

In summary, this study demonstrates the feasibility of quantitative multislice mapping of the myelin water fraction using multicompartment analysis of the T_2^* decay. A 3-pool model can be effectively used to assess the MR signal arising from the myelin water, myelinated axon water, and mixed water in fixed brains at 3T. Using this method, multislice data acquisition can be completed in a clinically acceptable scan time.

ACKNOWLEDGMENTS

The authors thank the Rocky Mountain Multiple Sclerosis Bank for providing the MS brain, Ms. Lisa Litzenberger for photographic expertise, and Bernadette Sullivan, Dr. Cathy Adams, and Dr. Sherry Leonard for providing the non-MS fixed brains.

REFERENCES

1. Menon RS, Rusinko MS, Allen PS. Proton relaxation studies of water compartmentalization in a model neurological system. Magn Reson Med 1992;28:264–274.
2. MacKay A, Whittall K, Adler J, Li D, Paty D, Graeb D. In vivo visualization of myelin water in brain by magnetic resonance. Magn Reson Med 1994;31:673–677.
3. Levitt MH, Freeman R. NMR population inversion using a composite pulse. J Magn Reson 1979;33:473.
4. Poon CS, Henkelman RM. Practical T2 quantitation for clinical applications. J Magn Reson Imaging 1992;2:541–553.
5. Whittall KP, MacKay AL. Quantitative interpretation of NMR relaxation data. J Magn Reson 1989;84:134–152.
6. Whittall KP, MacKay AL, Li DK, Vavasour IM, Jones CK, Paty DW. Normal-appearing white matter in multiple sclerosis has heterogeneous, diffusely prolonged T_2. Magn Reson Med 2002;47:403–408.
7. Lancaster JL, Andrews T, Hardies LJ, Dodd S, Fox PT. Three-pool model of white matter. J Magn Reson Imaging 2003;17:1–10.
8. Andrews T, Lancaster JL, Dodd SJ, Contreras-Sesvold C, Fox PT. Testing the three-pool white matter model adapted for use with T_2 relaxometry. Magn Reson Med 2005;54:449–454.
9. Posse S, Dager SR, Richards TL, Yuan C, Ogg R, Artru AA, Muller-Gartner HW, Hayes C. In vivo measurement of regional brain metabolic response to hyperventilation using magnetic resonance: proton echo planar spectroscopic imaging (PEPSI). Magn Reson Med 1997;37:858–865.
10. Pauly J, LeRoux P, Macovski A. Parameter relations for the Shinnar-Le Roux selective excitation pulse design algorithm. IEEE Trans Med Imaging 1991;10:53.
11. Du W, Du YP, Fan X, Zamora MA, Karczmar GS. Reduction of spectral ghost artifacts in high-resolution echo-planar spectroscopic imaging of water and fat resonances. Magn Reson Med 2003;49:1113–1120.
12. Moore GR, Leung E, MacKay AL, Vavasour IM, Whittall KP, Cover KS, Li DK, Hashimoto SA, Oger J, Sprinkle TJ, Paty DW. A pathology-MRI study of the short-T_2 component in formalin-fixed multiple sclerosis brain. Neurology 2000;55:1506–1510.
13. Whittall KP, MacKay AL, Graeb DA, Nugent RA, Li DK, Paty DW. In vivo measurement of T_2 distributions and water contents in normal human brain. Magn Reson Med 1997;37:34–43.
14. Laule C, Vavasour IM, Moore GR, Oger J, Li DK, Paty DW, MacKay AL. Water content and myelin water fraction in multiple sclerosis. A T_2 relaxation study. J Neurol 2004;251:284–293.
15. Jones CK, Xiang QS, Whittall KP, MacKay AL. Linear combination of multiecho data: short T2 component selection. Magn Reson Med 2004; 51:495–502.
16. Oh J, Han ET, Pelletier D, Nelson SJ. Measurement of in vivo multicomponent T2 relaxation times for brain tissue using multi-slice T2 prep at 1.5 and 3 T. Magn Reson Imaging 2006;24:33–43.
17. Henkelman RM. Measurement of signal intensities in the presence of noise in MR images. Med Phys 1985;12:232–233.
18. Hu X, Kim SG. Reduction of signal fluctuation in functional MRI using navigator echoes. Magn Reson Med 1994;31:495–503.